

Figure S1 Evaluating our *in cellulo* mammalian cell culture system. **a**, Determination of number of UASs in the artificial promoter to regulate the output reporter gene. We first constructed reporter vectors, varying the number of UAS (from 1 through 5) on the promoter driving a reporter gene (*dLuc*). We transfected them with a morning activator and a night-time repressor into NIH3T3 cells and then monitored the bioluminescence from the cells. The raw bioluminescence data from two independent samples are shown. The relative amplitudes of each output signal from two independent samples are also shown (**lower left panel**). **b**, Determination of number of CCEs in the artificial promoter to regulate the activator and repressor genes. We first constructed two sets of vectors with two and three copies of the clock-controlled elements (CCE; E'-box from the *Per2* gene, or RRE from the *Bmal1* gene) on promoters driving a reporter gene (*dLuc*), an artificial activator gene (*dGal4-VP16*) or an artificial repressor gene (*dGal4*). We then monitored their promoter activities (either 2x or 3x E'-box, and either 2x or 3x RRE) as well as the output

(UAS) from artificial transcriptional circuits with a morning activator and a night-time repressor. The raw bioluminescence data from two independent samples are shown. The relative amplitudes of each output signal from two independent samples are also shown (**lower left panel**). **c**, Negative controls for quantification of GAL4-VP16-FLAG and GAL4-FLAG bindings to the UAS in the artificial transcriptional circuits. After normalization for the amount of input DNA, the amount of *Tbp*-5' promoter (*Tbp*-5') region immunoprecipitated by anti-FLAG antibody (squares) and by anti-V5 antibody (triangles) were quantified relative to a constitutively unbound region (*Act5'*). These relative amounts of *Tbp*-5' ChIP products are indicated along with the LUC activity (line) for two different artificial transcriptional circuits using dGAL4-VP16-FLAG (green) and dGAL4-FLAG (magenta). ChIP assays were performed with the artificial transcriptional circuit (morning activator and night-time repressor) in NIH3T3 cells at 4-h intervals for 24 h with anti-FLAG antibody and anti-V5 antibody as negative control.

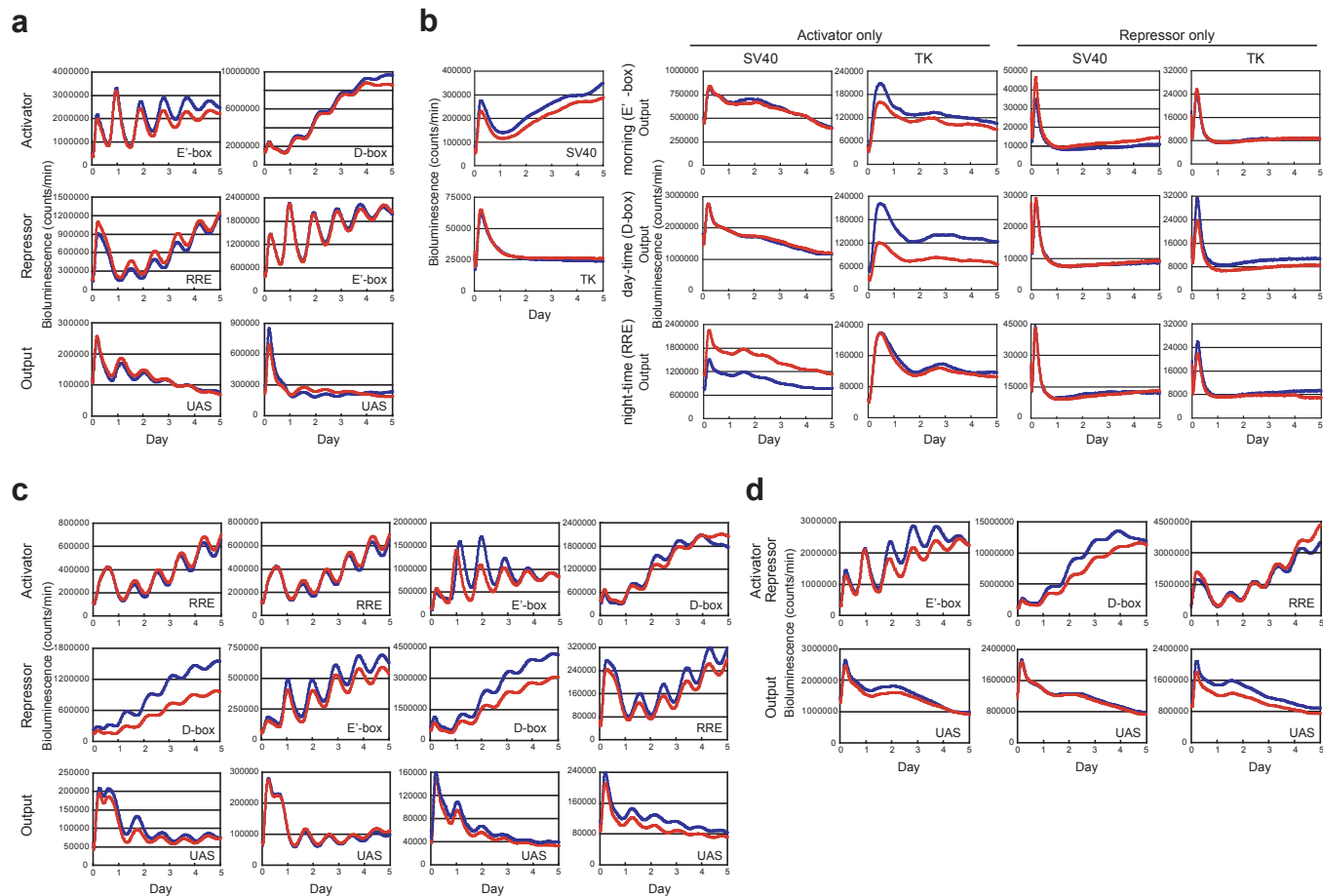


Figure S2 Raw bioluminescence data from artificial transcriptional circuits with various combinations of activators and repressors. **a**, Synthesis of day-time and night-time expressions in two different artificial transcriptional circuits. Promoter activities of an activator, repressor, and output reporter in two different artificial transcriptional circuits: **(left)** morning activator under E'-box control and night-time repressor under RRE control, and **(right)** day-time activator under D-box control and morning repressor under E'-box control. **b**, High-amplitude transcriptional oscillation cannot be generated by an activator or a repressor alone. **(left)** The activities of the SV40 promoter and thymidine kinase (TK) promoter. The promoter activities were monitored by bioluminescence from NIH3T3 cells, which were transfected SV40-*dLuc* and TK-*dLuc*. The transcriptional activity of TK promoter indicates lower expression than SV40 promoter ($1:7.28 \pm 0.70$). **(right)** Promoter activities of the output reporter in six different artificial transcriptional circuits. The promoters used to regulate the activator and repressor genes were SV40 promoter (SV40, **left panels**) and TK promoter (TK, **right panels**): morning activator or repressor alone (**upper**

panels), day-time activator or repressor alone (**middle panels**) and night-time activator or repressor alone (**lower panels**). **c**, Synthesis of various circadian phases from three basic circadian phases in artificial transcriptional circuits. Promoter activities of an activator, a repressor, and an output reporter in four different artificial transcriptional circuits: **(left)** night-time activator under RRE control and day-time repressor under D-box control, **(middle left)** night-time activator under RRE control and morning repressor under E'-box control: **(middle right)** morning activator under E'-box control and day-time repressor under D-box control: and **(right)** day-time activator under D-box control and night-time repressor under RRE control. **d**, Promoter activity in phase with an activator. Promoter activities of an activator, repressor, and output reporter in three different artificial transcriptional circuits: **(left)** morning activator and repressor both under E'-box control: **(middle)** day-time activator and repressor both under D-box control: and **(right)** night-time activator and repressor both under RRE control. The raw bioluminescence data from two independent samples are shown.

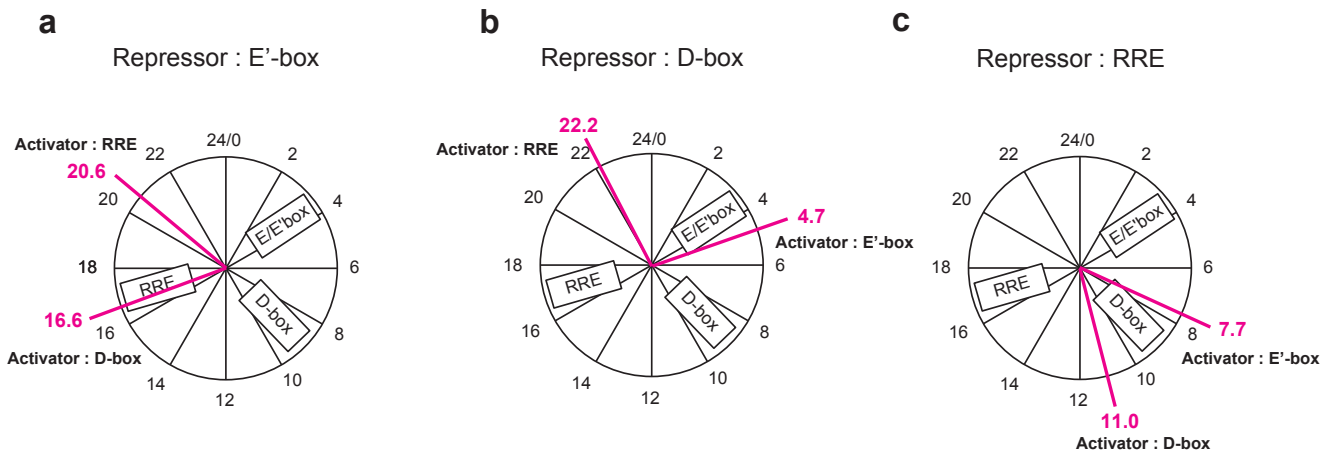


Figure S3 Transcriptional mechanisms to generate novel phases. Output phases in artificial transcriptional circuits with a morning repressor (a), day-time repressor (b), or night-time repressor (c). The phase of an output reporter (magenta lines and numbers) is indicated in circadian

time (h) with the activator used (bold black). In artificial transcriptional circuits *in cellulo*, the output phase could be changed according to the input phase of the activator, even if that of the repressor was unchanged.

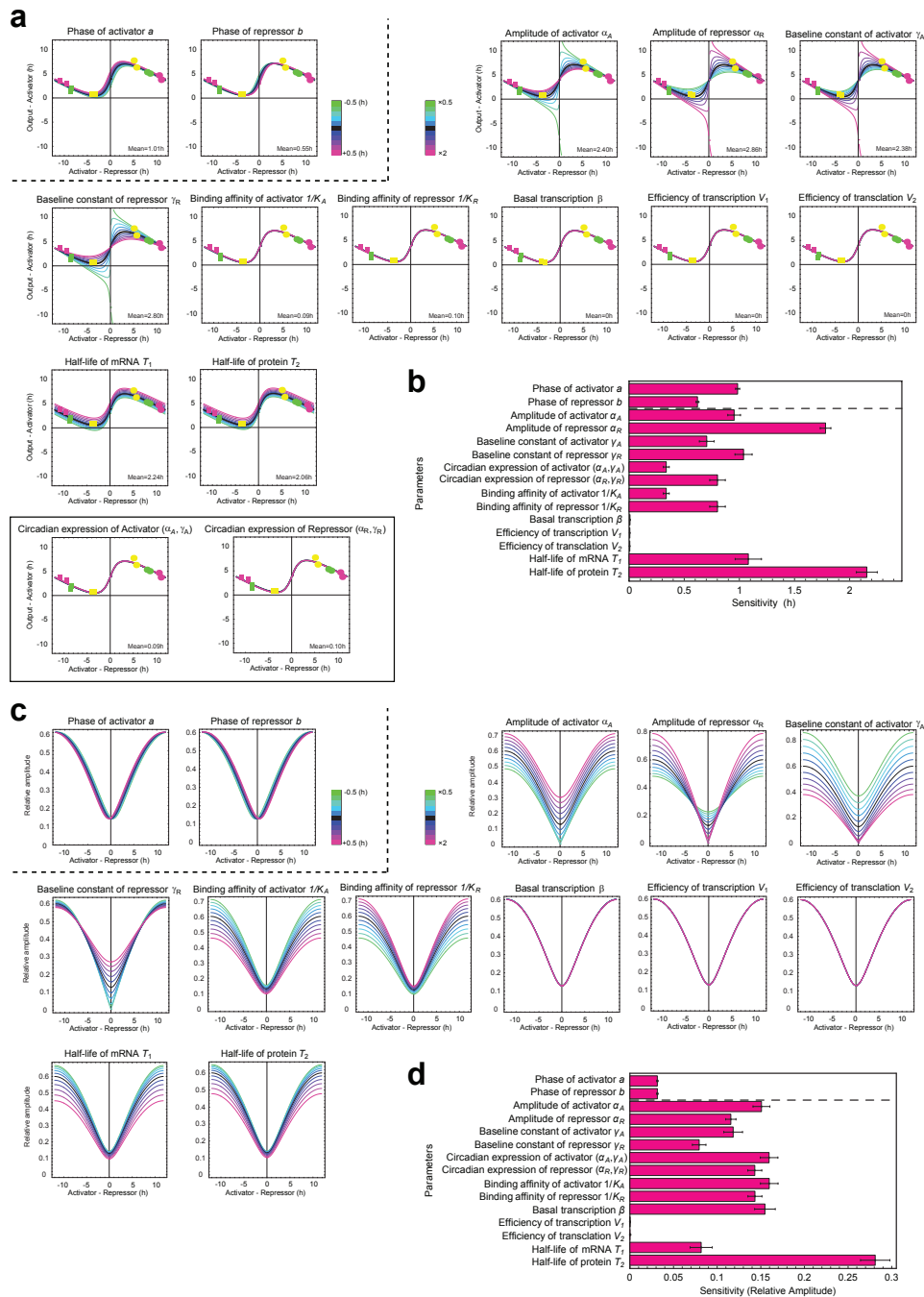


Figure S4 Sensitivity of the output phase and the relative amplitude to each parameter. **a**, The sensitivity of the output phase over $-12 < a-b < 12$ is shown when each parameter value was changed by 1 hour (a and b) or 4-fold (the others). X-axis represents the advance of a repressor compared to an activator (h) (phase difference between an activator and repressor), while Y-axis represents the delay of an output reporter compared to an activator (h) (phase difference between an output reporter and activator). The effects of simultaneous increases in both absolute amplitude and base-line levels of an input activator (α_A and γ_A) or repressor (α_R and γ_R) are also shown in the boxed-panel (**inb**ox). The black curve shows a simulation model with representative parameter values of one hundred fitted parameter sets; the other curves show changed values for sensitive analysis. **b**, The simulated sensitivity of the output phase to the parameter describing each process. Each bar shows the average phase difference obtained by changing its original parameter value by 1 hour (parameter a and b) or 4-fold (other

parameters). Each error bar represents standard error. These values were calculated from 100 simulations with trimming of the 5% outliers. **c**, The sensitivity of the relative amplitude over $-12 < a-b < 12$ is shown when each parameter value was changed by 1 hour (a and b) or 4-fold (the others). X-axis represents the advance of a repressor compared to an activator (h) (phase difference between an activator and repressor), while Y-axis represents the relative amplitude of oscillation of output protein (dLUC) activity. The black curve shows a simulation model with representative parameter values of one hundred fitted parameter sets; the other curves show changed values for sensitive analysis. **d**, The simulated sensitivity of the relative amplitude to the parameter describing each process. Each bar shows the average relative amplitude difference obtained by changing its original parameter value by 1 hour (parameter a and b) or 4-fold (other parameters). Each error bar represents standard error. These values were calculated from 100 simulations with trimming of the 5% outliers.

Supplementary Text

Determination of number of the galactose upstream activating sequences.

The number of the galactose upstream activating sequences (UASs) was determined by the following experiments. We constructed reporter vectors with varying numbers of UAS (from 1 through 5) on the promoter driving *dLuc* output, reporter, transfected the vector into NIH3T3 cells and then monitored bioluminescence from the transfected cells (**Supplementary Fig. 1a**). We observed that reporter vectors with 1 or 2×UAS did not exhibit high-amplitude oscillations, while those with 3, 4, and 5×UAS produced high-amplitude oscillations in comparable phases. In this manuscript, we adopt 4×UAS because outputs with 4×UAS results in the relative amplitudes with the smallest variation (**Supplementary Fig. 1a lower left**).

Determination of number of the clock-controlled elements.

To determine the number of clock-controlled elements (CCE) that we should use to drive activator/repressor expression, we constructed two sets of vectors containing either two or three copies of the CCEs on promoters driving *dLuc* reporter or artificial activators/repressors, and monitored their promoter activities and transcriptional output (**Supplementary Fig. 1b**). Via bioluminescence, we observed that promoter activities and outputs for both 2 and 3×CCE exhibited comparable phases and relative amplitudes (**Supplementary Fig. 1b lower left**). Although we could have used 2×CCE, we opted to use 3×CCE in our system, because it has been the construct used since our preceding works¹.

Comparison of the previous predictions and the numerical experimental data

The predictions of repressor-antiphase-to-activator and repressor-precedes-activator mechanisms in the previous report¹ is well matched with our numerical experimental data although we should give attention to the difference of the transcription activity that was evaluated in the previous model and the output protein activities that were measured in our experiment. Due to transcription and translation of an output reporter, the simulation model with representative parameter values (**black line in Fig. 5a**) in our current manuscript has an approximately 4-hour delay from the previous model. This delay is comparable to the delay estimated from our experiment in **Fig. 2a** and **b**, where the peak-time of dGAL4-VP16 binding to UAS and peak-time of *Luciferase* mRNA are about 3.0-hour and 2.0-hour before that of output *Luciferase* activity, respectively, and thus the delay between transcription activity and output protein was estimated as about 2.0–3.0 hours.

Sensitivity analysis of the phase and relative amplitude of the output oscillations

We calculated the sensitivity of the phase and the relative amplitude of the output oscillation to each parameter by changing the parameter's value by 4-fold (from 1/2- to 2-times the original parameter value) (**Supplementary Fig. 4a, c**), *except* for the input phase of the transcriptional factors, which we changed by 1 h (from a 0.5-h delay to 0.5-h in advance of the original phase). By repeating this procedure for 100 fitted parameter sets, we also evaluated the average contribution of each process (**Supplementary Fig. 4b, d**).

As expected from our *in cellulo* mammalian cell culture system results (**Figs. 4a-c**), the phase difference of input transcription factors can contribute to the output phase *in silico* (**Supplementary Fig. 4b**). For example, a 1-h alteration in the phase of an activator or a repressor led to ~ 1 h changes in the output phase (0.98 h for a and 0.62 h for b). In addition, the absolute amplitude and base-line level of the input transcription factor phases contributed to the output phase: a 4-fold parameter change in the absolute amplitude (α_A and α_R) or the absolute base-line level (γ_A and γ_R) of an activator or repressor could alter the output phase by 1 \sim 2 h (0.95 h for α_A , 1.77 h for α_R , 0.70 h for γ_A and 1.03 h for γ_R). However, the effects of absolute amplitudes and base-line levels on output phase seemed to cancel out when they were both increased simultaneously. This was because the effects of simultaneous increases of *both* absolute amplitude and base-line levels of the inputs are smaller than *independent* increases in absolute amplitude *or* base-line levels (0.33 h for α_A and γ_A , and 0.80 h for α_R and γ_R and see also **Supplementary Fig. 4a inbox**). We noted that binding affinities of the input activator or repressor onto the promoters ($1/K_A$, or $1/K_R$) are theoretically equivalent to the simultaneous increase of α_A and γ_A , or α_R and γ_R , respectively (0.33 h for $1/K_A$ and 0.80 h for $1/K_R$). We also noted that the half-life of the mRNA or protein of a reporter (1.07 h for T_1 and 2.14 h for T_2) contributed more to the output phase than the reporter's transcription or translation processes (<0.01 h for β , V_1 and V_2), which implies that the degradation process can cause output phases to be fairly continuous, as is observed *in vivo*²⁻⁵.

As for the contribution of input transcription factors to the relative amplitude of the output oscillations (**Supplementary Fig. 4d**), we find that the absolute amplitudes and base-line levels of the inputs have larger effects than the phases of the inputs (0.15 for α_A , 0.12 for α_R , 0.12 for γ_A and 0.08 for γ_R , 0.03 for a , 0.03 h for b). Interestingly, these effects of absolute amplitudes and base-line levels of the inputs do not seem to

cancel out much when both are increased simultaneously since the effects of simultaneous increase of *both* absolute amplitude and base-line levels of the inputs are similar to, or greater than, those of *either* absolute amplitude or base-line levels of the inputs (0.16 for α_A and γ_A , and 0.14 for α_R and γ_R and see also **Fig. 5d**). Hence, we observe a marked contrast to the output phase, implying that absolute circadian expression levels of the inputs seem to play a key role in controlling the relative amplitudes of outputs.

To recap, we noted: 1) that binding affinity of the input activator or repressor onto the promoters ($1/K_A$, or $1/K_R$) are theoretically equivalent to the simultaneous increase of α_A and γ_A , or α_R and γ_R , respectively (0.16 for $1/K_A$ and 0.14 for $1/K_R$), and; 2) that the half-life of the mRNA or protein of a reporter (0.08 for T_I and 0.28 h for T_2) also contributed to the relative amplitude of the output. Interestingly, however, basal transcription is more important for the relative amplitude of the output than the efficiencies of transcription and translation (0.15 for β , <0.001 for V_I and V_2).

Supplementary Methods

Construction of pCMV-*dGal4-VP16-Flag* and pCMV-*dGal4-Flag*. To construct *Flag*-tagged activator and repressor plasmids regulated by CMV promoter, the *Flag*-PEST coding DNA fragment, amplified from the pCMV-*dGal4* plasmid (See **Methods** in main text) by PCR with forward (5'-GGCCGCAGGTACCGACTACAAGGATGACGATGACAAGAGCCATGGCTTCCCGCCGGCGGTG-3') and reverse (5'-TTATTCAGGTACCCACATTGATCCTAGCAGAAGC-3') primers containing the *KpnI* recognition sequence (under line) and *Flag* coding sequence (italics), was inserted into the *VP16*-fused and original pBIND vectors (Promega, See **Methods** in main text), previously digested with *KpnI*. These products were termed pCMV-*dGal4-VP16-Flag* and pCMV-*dGal4-Flag*, respectively, and used for Western Blot analysis.

Measurement of protein half-lives of dGAL4-VP16-FLAG and dGAL4-FLAG.

NIH3T3 cells (American Type Culture Collection) were grown in DMEM (Invitrogen) supplemented with 10% FBS (JRH Biosciences) and antibiotics (25 U/ml penicillin, 25 mg/ml streptomycin; Invitrogen). Cells were plated at 1×10^6 cells per dish in 90-mm dishes 24 h before transfection. These cells were transfected with FuGene6 (Roche) according to the manufacturer's instructions. The cells in each well were transfected with 12 μ g of pCMV-*dGal4-VP16-Flag* or pCMV-*dGal4-Flag*. After 24 h, the cells in each well were harvested and plated in 6 35-mm dishes. After 48 h, the cells were treated with cycloheximide (CHX, SIGMA) at a final concentration of 100 μ g/ml until their harvest. The treated cells were harvested at 0, 2, 4 and 6 h and used for Western Blot Analysis.

For Western Blot Analysis, each nuclear and cytoplasmic fraction was extracted from the harvested cells with NE-PER Nuclear and Cytoplasmic Extraction Reagents (PIERCE). Each cell lysate was applied to a lane of polyacrylamide gels. For immunoblot analysis, proteins were transferred to PVDF membranes. Anti-FLAG M2 monoclonal Antibody-Peroxidase Conjugate (SIGMA) was diluted 2000-fold and used for detection of dGAL4-VP16-FLAG and dGAL4-FLAG protein. Anti-Tubulin α monoclonal antibody (clone DM1A, LAB VISION) was diluted 330-fold, and used for detection of Tubulin α protein as internal control. For visualization, ECL Plus Western Blotting Detection System (GE Healthcare) and LAS-1000 (FUJIFILM) were used according to the manufacturer's instructions.

Construction of plasmid pG1-*dLuc*, pG2-*dLuc*, pG3-*dLuc* and pG5-*dLuc*. To construct the output reporter plasmids, the pG5*Luc* (containing five UAS) plasmid in the CheckMate Mammalian Two-Hybrid system (Promega) was modified to contain one, two or three tandem repeats of the galactose upstream activating sequences (UAS) and a gene encoding destabilized luciferase (*dLuc*) as follows. pG5*Luc* was digested with *Xba*I (partial digestion) and *Eco*RI (for remaining one UAS), *Xho*I and *Nhe*I (for remaining two UAS), or *Xho*I and *Eco*RI (for remaining three UAS). These digested vectors were blunted by T4 DNA Polymerase, and ligated with itself. The products and pG5*Luc* (Promega) were then digested with *Sph*I and *Sal*I, ligated to the *Sph*I-*Sal*I fragment from the SV40-*dLuc* plasmid, which contains the PEST sequence of the *dLuc*¹ and termed pG1-*dLuc* (containing one UAS), pG2-*dLuc* (containing two UAS), pG3-*dLuc* (containing three UAS), and pG5- *dLuc* (containing five UAS). These constructs were used as the reporter plasmids for the artificial transcription circuits.

Real-time circadian reporter assays using reporter vectors with UAS (1-5×).

Real-time circadian assays were performed as previously described^{1,6} with the following modifications. NIH3T3 cells (American Type Culture Collection) were grown in DMEM (Invitrogen) supplemented with 10% FBS (JRH Biosciences) and antibiotics (25 U/ml penicillin, 25 mg/ml streptomycin; Invitrogen). Cells were plated at 1×10^5 cells per well in 35-mm dishes 24 h before transfection. These cells were transfected with FuGene6 (Roche) according to the manufacturer's instructions. The cells in each well were transfected with three plasmids (0.4 μ g of *dLuc* reporter plasmid, 0.025 μ g of p3×E'-box-SV40-*dGal4-VP16*, and 0.1 μ g of p3×RRE-SV40-*dGal4*). As the *dLuc* reporter plasmid, we used p3×E'-box-SV40-*dLuc* and p3×RRE-SV40-*dLuc*¹ for monitoring the promoter activity of the artificial transcription factors, or pG1-*dLuc*, pG2-*dLuc*, pG3-*dLuc*, pG4-*dLuc*, and pG5-*dLuc* for monitoring the transcriptional output in the artificial transcriptional circuits. The amount of transfected plasmid was adjusted to 2.0 μ g with empty vector. After 72 h, the media in each well was replaced with 2 ml of culture medium (DMEM/10% FBS) supplemented with 10 mM HEPES (pH 7.2, Invitrogen), 0.1 mM luciferin (Promega), antibiotics, and 0.01 μ M forskolin (Nacalai Tesque). Bioluminescence was measured with photomultiplier tube (PMT) detector assemblies (LM2400, Hamamatsu Photonics). The modules and cultures were maintained in a darkroom at 30°C and interfaced with computers for continuous data acquisition. Photons were counted for 1 min at 12-min intervals.

Construction of plasmid p2×CCE-SV40-*dLuc*, p2×CCE-SV40-*dGal4-VP16* and p2×CCE-SV40-*dGal4*. To construct activator or repressor plasmids regulated by two tandem repeated clock-controlled element (CCE), we modified the pCMV-*dGal4-VP16* or pCMV-*dGal4* vectors as follows. The oligonucleotides containing two tandem repeat sequences of CCEs were annealed, and inserted into *MluI/BglIII* site of the

SV40-*dLuc* vectors¹. These products (p2×CCE-SV40-*dLuc* plasmids) were digested with *KpnI* and *HindIII*, blunted by T4 DNA polymerase, and inserted into the *BgIII* and *NheI* site of pCMV-*dGal4-VP16* or pCMV-*dGal4*. The end products, p2×CCE-SV40-*dGal4-VP16* or p2×CCE-SV40-*dGal4*, and the intermediate product p2×CCE-SV40-*dLuc* were used as the activator or repressor plasmids for the artificial transcription circuits, and as the reporter plasmid for promoter activity, respectively.

The oligonucleotide sequence for two tandem repeated clock-controlled element.

2× *Per2* E'-box-forward:

5'-CGCGGCGCGCGCGGTCACGTTTTTCCACTATGTGACAGCGGAGGGCGCGCG
CGGTCACGTTTTTCCACTATGTGACAGCGGAGG-3'

2× *Per2* E'-box-reverse:

5'-GATCCCTCCGCTGTCACATAGTGGAAAACGTGACCGCGCGCGCCCTCCGC
TGTCACATAGTGGAAAACGTGACCGCGCGCGC-3'

2× *Bmal1* RRE-forward:

5'-CGCGAGGCAGAAAGTAGGTCAGGGACGAGGCAGAAAGTAGGTCAGGGA
CG-3'

2× *Bmal1* RRE-reverse:

5'-GATCCGTCCCTGACCTACTTTCTGCCTCGTCCCTGACCTACTTTCTGCCT-3'

Real-time circadian reporter assays using artificial activator and repressor derived by 2×CCE-SV40 promoters. Real-time circadian assays were performed as previously described^{1,6} and as mentioned above with the following modifications.

NIH3T3 cells were plated at 1×10^5 cells per well in 35-mm dishes 24 h before transfection, and were transfected with FuGene6. The cells in each well were transfected with three plasmids (0.4 μg of *dLuc* reporter plasmid, 0.025 μg of p2 \times E'-box-SV40-*dGal4-VP16*, and 0.1 μg of p2 \times RRE-SV40-*dGal4*). As the *dLuc* reporter plasmid, we used p2 \times E'-box-SV40-*dLuc* and p3 \times RRE-SV40-*dLuc*¹ for monitoring the promoter activity of the artificial transcription factors, and pG4-*dLuc* for monitoring the transcriptional output in artificial transcriptional circuits. The amount of transfected plasmid was adjusted to 2.0 μg with empty vector. After 72 h, the media in each well was replaced with 2 ml of culture medium including 0.01 μM forskolin. Bioluminescence was measured with photomultiplier tube (PMT) detector assemblies (LM2400) in a darkroom at 30°C.

Construction of p3 \times E'-box-SV40-*dGal4-VP16-Flag* and

p3 \times RRE-SV40-*dGal4-Flag*. To construct *Flag*-tagged activator and repressor plasmids regulated by E'-box and RRE, the *Flag*-PEST coding DNA fragment, amplified from the pCMV-*dGal4* plasmid (See **Methods** in main text) by PCR with forward

(5'-GGCCGCAGGTACCGACTACAAGGATGACGATGACAAGAGCCATGGCTTCCCGCCGGCGGTG-3') and reverse

(5'-TTATTCAGGTACCCACATTGATCCTAGCAGAAGC-3') primers containing the *KpnI* recognition sequence (under line) and *Flag* sequence (italics), was inserted into the *KpnI* sites of p3 \times E'-box-SV40-*dGal4-VP16* and p3 \times RRE-SV40-*dGal4* vectors (See **Methods** in main text), that were previously digested with *KpnI*. These products were termed p3 \times E'-box-SV40-*dGal4-VP16-Flag* and p3 \times RRE-SV40-*dGal4-Flag*, and used for Chromatin Immunoprecipitation assay.

Chromatin Immunoprecipitation (ChIP) assay and Quantitative PCR of ChIP

product. NIH3T3 cells (American Type Culture Collection) were grown in DMEM (Invitrogen) supplemented with 10% FBS (JRH Biosciences) and antibiotics (25 U/ml penicillin, 25 mg/ml streptomycin; Invitrogen). Cells were plated at 1×10^6 cells per dish in 14 90-mm dishes 24 h before transfection. These cells were transfected with FuGene6 (Roche) according to the manufacturer's instructions. The cells in each dish were transfected with three plasmids ($\{8 \mu\text{g}$ of pG4-*dLuc*, $4.8 \mu\text{g}$ of p3 \times E'-box-SV40-*dGal4-VP16-Flag* and $19.2 \mu\text{g}$ of p3 \times RRE-SV40-*dGal4* $\}$ and $\{8 \mu\text{g}$ of pG4-*dLuc*, $4.8 \mu\text{g}$ of p3 \times E'-box-SV40-*dGal4-VP16* and $19.2 \mu\text{g}$ of p3 \times RRE-SV40-*dGal4-Flag* $\}$). After 24 h, the cells in each well were harvested and plated in 14 90-mm dishes and two 35-mm dishes. After 48 h, the media in each dish was replaced with 10 ml of culture medium (DMEM/10% FBS) supplemented with 10 mM HEPES (pH 7.2, Invitrogen), antibiotics, and $0.01 \mu\text{M}$ forskolin (Nacalai Tesque), and cultured at 30°C . After 12, 16, 20, 24, 28, 32, 36 h from the stimulation, the treated cells were fixed with 1% paraformaldehyde by a set of two dishes and used for Chromatin Immunoprecipitation. In the same time, bioluminescence was measured with photomultiplier tube (PMT) detector assemblies (LM2400, Hamamatsu Photonics) with the cells in 35-mm dishes, which was replaced with 2 ml of culture medium (DMEM/10% FBS) supplemented with 10 mM HEPES (pH 7.2, Invitrogen), 0.1 mM luciferin (Promega), antibiotics, and $0.01 \mu\text{M}$ forskolin (Nacalai Tesque). The modules and cultures were maintained in a darkroom at 30°C and interfaced with computers for continuous data acquisition. Photons were counted for 1 min at 12-min intervals.

Chromatin Immunoprecipitation assays with these NIH3T3 cells were performed as previously described⁷ with the following modifications. In this report,

we used Chromatin Immunoprecipitation Assay Kits (Upstate Biotechnology), anti-FLAG M2 antibody (Sigma) and anti-V5 antibody (Sigma). Protein G-Sepharose (GE Healthcare) was used for precipitation of antibody/protein immune complexes. The resulting precipitated DNA was quantified by quantitative PCR. Quantitative PCR was performed using ABI Prism 7700 and Power SYBR Green Reagents (Applied Biosystems). Samples contained 1×Power SYBR Green Master Mix (Applied Biosystems), 0.5 μM primers and 1/25 ChIP product DNA in a 10 μl volume. The PCR conditions were as follows: 10 min at 95°C, then 45 cycles of 15 s at 94°C, 30 s at 59°C and 1 min at 72°C. Absolute DNA abundance was calculated using the standard curve obtained from NIH3T3 cell's genomic DNA and pG4-*dLuc* plasmid. The *Act* promoter (*Act*-5') and *Tbp* promoter (*Tbp*-5') regions were used as the internal control.

Primer sequence for Quantitative PCR of ChIP product.

UAS-forward: 5'-TAGGCTGTCCCCAGTGCAAG-3'

UAS-reverse: 5'-CGATAGAGAAATGTTCTGGCAC-3'

Act-5'-forward: 5'-CCAAGAGGCTCCCTCCACA-3'

Act-5'-reverse: 5'-GTGCAAGGGAGAAAGATGCC-3'

Tbp-5'-forward: 5'-GAGAGCATTGGACTCCCCAG-3'

Tbp-5'-reverse: 5'-AGCACCCACATGGCTACTCAC-3'

Quantitative PCR of *dLuc* mRNA. NIH3T3 cells were transfected on the same condition as ChIP assay (as described above), and harvested at same timing of ChIP assay. Total RNAs were purified from the harvested cells using TRIzol reagent (Invitrogen), and treated with DNaseI with RNeasy kit (QIAGEN) and RNase-free

DNase set (QIAGEN) according to the standard protocol. The cDNA was synthesized from 0.25 µg of total RNA with random 6mer (Promega) and Superscript II Reverse Transcriptase (Invitrogen) according to the standard protocol. Quantitative PCR was performed using ABI Prism 7700 and Power SYBR Green Reagents (Applied Biosystems). Samples contained 1×Power SYBR Green Master Mix (Applied Biosystems), 0.5 µM primers and 1/20 synthesized cDNA in a 10 µl volume. The PCR conditions were as follows: 10 min at 95°C, then 45 cycles of 15 s at 94°C, 30 s at 59°C and 1 min at 72°C. Absolute cDNA abundance was calculated using the standard curve obtained from NIH3T3 cell's genomic DNA and pG4-*dLuc* plasmid. *Gapdh* mRNA expression levels were quantified and used as the internal control.

Primer sequence for Quantitative PCR of mRNA.

Luciferase-forward: 5'-CTTACTGGGACGAAGACGAACAC-3'

Luciferase-reverse: 5'-GAGACTTCAGGCGGTCAACG -3'

Gapdh-forward: 5'-CAAGGAGTAAGAAACCCTGGACC-3'

Gapdh-reverse: 5'-CGAGTTGGGATAGGGCCTCT-3'

Peak-time estimation of transcription factors' binding and *Luciferase* mRNA.

First, we chose the largest points in the latter 4 time points (24 h - 36 h) for the dGAL4-VP16-FLAG ChIP and the *Luciferase* mRNA experiments, and the largest point in the former 4 time points (12 h - 24 h) for the dGAL4-FLAG ChIP experiment. Next, we fitted a quadratic function to 3 time points around the largest point for each experiment, and identified the top of the function as a peak-time of the experiment. The peak-times were converted into circadian time by using periods of simultaneously

measured Luciferase activities (21.66 for the *Luciferase* mRNA experiments, and 20.92 for the ChIP experiments), by the function: (the raw peak-time / the period of the *Luciferase* activity) * 24.

Construction of plasmid p3×CCE-TK-*dGal4-VP16* and p3×CCE-TK-*dGal4*. To construct activator or repressor plasmids regulated by thymidine kinase (TK) promoter, we modified the pCMV-*dGal4-VP16* or pCMV-*dGal4* vectors as follows. We amplified the TK promoter sequences from pMU2-P(TK) (unpublished, the origin of TK promoter was phRL-TK (Promega)) by PCR with a forward primer containing an *Bgl*III recognition sequence (5'-ATATATAGATCTCTAGCCCCGGGCTCGAGATC-3') and a reverse primer containing a *Nhe*I recognition sequence (5'-GTAGTAGCTAGCCCGTTATAGTTACTGCAGAAGC-3'). The PCR product was then digested with *Bgl*III and *Nhe*I, and inserted in the pCMV-*dGal4-VP16* or pCMV-*dGal4* vectors, that were previously digested with *Bgl*III and *Nhe*I. To drive the artificial activator or repressor by CCE, the oligonucleotides containing three tandem repeat sequences of CCEs were annealed, and inserted into *Bgl*III site of the pTK-*dGal4-VP16* or pTK-*dGal4* vectors. The end products, p3×CCE-TK-*dGal4-VP16* and p3×CCE-TK-*dGal4* plasmids, were used as the activator or repressor plasmids for the artificial transcription circuits.

The oligonucleotide sequence for three tandem repeated clock-controlled element.

3× *Per2* E'-box-forward:

5'-GATCGCGCGCGCGGTCACGTTTTCCACTATGTGACAGCGGAGGGCGCGCG

CGGTCACGTTTTCCACTATGTGACAGCGGAGGGCGCGCGCGGTCACGTTTTTC
CACTATGTGACAGCGGAG-3'

3× *Per2* E'-box-reverse:

5'-GATCCTCCGCTGTCACATAGTGGAAAACGTGACCGCGCGCGCCCTCCGCT
GTCACATAGTGGAAAACGTGACCGCGCGCGCCCTCCGCTGTCACATAGTGG
AAAACGTGACCGCGCGCGC-3'

3× *Per3* D-box-forward:

5'-GATCCCCGCGCGTTATGTAAGGTACTCGCCCGCGCGTATGTAAGGTACT
CGCCCGCGCGTATGTAAGGTACTCG-3'

3× *Per3* D-box-reverse:

5'-GATCCGAGTACCTTACATAACGCGCGGGCGAGTACCTTACATAACGCGCG
GGCGAGTACCTTACATAACGCGCGGG-3'

3× *Bmal1* RRE-forward:

5'-GATCAGGCAGAAAGTAGGTCAGGGACGAGGCAGAAAGTAGGTCAGGGA
CGAGGCAGAAAGTAGGTCAGGGACG-3'

3× *Bmal1* RRE-reverse:

5'-GATCCGTCCCTGACCTACTTTCTGCCTCGTCCCTGACCTACTTTCTGCCTC
GTCCCTGACCTACTTTCTGCCT-3'

Re-annotation of clock-controlled genes. The previously published genome-wide expression data for the liver ² were re-analyzed and re-annotated to find transcription factors that showed circadian expression. Each probe set that was identified as a clock-controlled gene in the previous report ², was annotated by using link information

in the Entrez Gene database (gene name, gene symbol, and Entrez Gene ID), link information in the TRANSFAC database (FACTOR, MATRIX, consensus binding sites, CLASS ID, and upstream transcription factors), the Affymetrix annotation file (InterPro ID), and information in the mammalian promoter/enhancer database (clock-controlled elements, E-box, D-box, and RRE) (Kumaki *et al.*, submitted). The annotation table is shown in **Supplementary Table 1** online.

Parameter search. First, the initial parameter set in the formulas of our theoretical model was randomly chosen except for K_A , K_R ($=1/2$), a ($=0$), b and n ($=1$). As multiplying by K_A , K_R is equivalent to dividing by both α_A , α_R and γ_A , γ_R , in the formula $T(t)$, K_A and K_R were fixed to a constant ($1/2$) to eliminate ambiguity. If the minimum amplitude of an output with a specific initial parameter set (obtained by changing the phase of the repressor) was too low or too high ($<1/100$ or >100 -fold of a mean amplitude of an activator and a repressor), the initial parameter set was discarded and a new parameter set was randomly searched again.

Second, one parameter other than K_A , K_R , a , b , n was chosen, and then ten different values of the parameter were generated within 30-fold of its original value. For each value of the parameter, graphs like that in **Fig. 5a** and **b** were drawn by changing the value of b . The first graph (**Fig. 5a**) shows relationships between phase differences of the activator and the repressor (activator phase – repressor phase) and phase differences of the activator and the output protein (output protein phase – activator phase). The second graph (**Fig. 5b**) shows relationships between phase difference of the activator and the repressor and the relative amplitude of the output protein. The points in these graphs represent observed outputs of various combinations of activators and repressors. The parameter value that had the lowest

least squares distance to the measured experimental points was chosen as the new value of the parameter. We did not use *-marked points because these outlier points have larger (>4-fold amounts of the activator than the repressor) differences between amounts of the activator and the repressor (**Fig. 5c**), and also seem to have lower relative amplitudes. This second fitting procedure was repeated until no more improvements were observed, and the final parameter set was recorded as a fitted parameter set. By repeating these procedures, we found 100 fitted parameter sets.

Sensitivity analysis. All parameters except for n were analyzed for the degree to which the output phase and the relative amplitude was sensitive to them. To calculate the sensitivity of the output phase to a certain parameter, the value of the parameter was changed within 1 hour (0.5-hour advance and 0.5-h delay) for a or b , or changed within a 4-fold (one-half and double the original parameter value) if it was one of the other parameters. For each parameter change, the maximum changes in phase difference between the activator and the output were calculated for each b within $-12 < b < 12$, and the average value of the maximum phase change (or the change of the relative amplitude) was calculated over $-12 < b < 12$ and defined as the "phase change" (or "relative amplitude change") due to the parameter change. This procedure was performed for each parameter set in 100 fitted parameter sets. The average and SEM of the phase change due to the parameter change were then calculated over the 100 fitted parameter sets with trimming of the 5% outliers, and defined as the measures of sensitivity of the corresponding parameter change.

Construction of p3×E'-box-SV40-*Dbp* and p3×RRE-SV40-*E4bp4*. To construct *Dbp* and *E4bp4* gene expression vectors regulated by E'-box and RRE, the *Dbp* and

E4bp4 coding sequence were amplified from the pMU2-*Dbp* and pMU2-*E4bp4* plasmids (Kumaki *et al.*, submitted) by PCR with forward (5'-CTCGAAGGAGAGGCCACCATGGAC-3') and reverse (5'-GCACCCGACATAGATTCATTAACCC-3') primers, and phosphorylated by Mighty Cloning kit <Blunt End> (TaKaRa). The vectors for insertion of these PCR fragment were amplified from the p3×E'-box-SV40-*dGal4* and p3×RRE-SV40-*dGal4* plasmids (See **Methods** in main text) by invert PCR with forward (5'-GGTACCTGAATAACTAAGGCCGCTTCC-3') and reverse (5'-CAGGAGGCTTGCTTCAAGCTGGC-3') primers, and blunted by T4 DNA Polymerase, and then dephosphorylated by Bacterial Alkaline Phosphatase. The *dGal4* coding region was deleted by this treatment. The *Dbp* and p3×E'-box-SV40 PCR fragments, and *E4bp4* and p3×RRE-SV40 PCR fragments were ligated, respectively. These products were termed p3×E'-box-SV40-*Dbp* and p3×RRE-SV40-*E4bp4*, and used for perturbation experiment.

Perturbation experiments of natural transcriptional circuits to verify the predictions. Real-time circadian assays were performed as previously described^{1,6} with the following modifications. NIH3T3 cells (American Type Culture Collection) were grown in DMEM (Invitrogen) supplemented with 10% FBS (JRH Biosciences) and antibiotics (25 U/ml penicillin, 25 mg/ml streptomycin; Invitrogen). Cells were plated at 1×10^5 cells per well in 35-mm dishes 24 h before transfection. These cells were transfected with FuGene6 (Roche) according to the manufacturer's instructions. The cells in each well were transfected with two plasmids (0.5 μ g of p3×D-box-SV40-*dLuc*¹ reporter plasmid, 0, 0.1, 0.3, 0.6, 0.9, 1.2, 1.5 μ g of p3×E'-box-SV40-*Dbp* or p3×RRE-SV40-*E4bp4*). The amount of transfected plasmid was adjusted to 2.0 μ g with empty vector. After 72 h, the media in each well was

replaced with 2 ml of culture medium (DMEM/10% FBS) supplemented with 10 mM HEPES (pH 7.2, Invitrogen), 0.1 mM luciferin (Promega), antibiotics, and 0.01 μ M forskolin (Nacalai Tesque). Bioluminescence was measured with photomultiplier tube (PMT) detector assemblies (LM2400, Hamamatsu Photonics). The modules and cultures were maintained in a darkroom at 30°C and interfaced with computers for continuous data acquisition. Photons were counted for 1 min at 12-min intervals.

References

1. Ueda, H.R. et al. System-level identification of transcriptional circuits underlying mammalian circadian clocks. *Nat Genet* **37**, 187-192 (2005).
2. Ueda, H.R. et al. A transcription factor response element for gene expression during circadian night. *Nature* **418**, 534-539 (2002).
3. Akhtar, R.A. et al. Circadian cycling of the mouse liver transcriptome, as revealed by cDNA microarray, is driven by the suprachiasmatic nucleus. *Curr Biol* **12**, 540-50 (2002).
4. Panda, S. et al. Coordinated transcription of key pathways in the mouse by the circadian clock. *Cell* **109**, 307-20 (2002).
5. Storch, K.F. et al. Extensive and divergent circadian gene expression in liver and heart. *Nature* **417**, 78-83 (2002).
6. Sato, T.K. et al. Feedback repression is required for mammalian circadian clock function. *Nat Genet* **38**, 312-319 (2006).
7. Yamashita, M. et al. Identification of a Conserved GATA3 Response Element Upstream Proximal from the Interleukin-13 Gene Locus. *J. Biol. Chem.* **277**, 42399-42408 (2002).